A *UDEC* model for "kink band slumping" type failures of rock slopes

A. Preh & R. Poisel
Institut for Engineering Geology, Vienna University of Technology, Vienna, Austria

ABSTRACT: The term "kink band slumping" introduced by Kieffer (1989) describes a failure mechanism of rock slopes and valley flanks when bedding planes or foliation joints, dipping into the same direction as the slope but not daylighting, form thin rock lamellae. These lamellae undergo large S-shaped deformations during the slope displacements. According to Kieffer the mechanism is composed of the modes "toppling" and "rock slumping". However, due to the deformation pattern the mechanisms "buckling" and "slope creep" might also be involved. Thus a numerical model, allowing large deformations of the rock due to viscoplastic behavior as well as large shear displacements between the lamellae, has to be built up in order to assess the stability of such slopes. This was realized by means of the Distinct Element Method code, *UDEC*, with a Mohr-Coulomb model for the material. In order to improve the plastic flow calculation of the *UDEC*-model, diagonally opposed triangular zones have been used for the zoning within the blocks. These analyses showed that no influence of buckling could be found and "kink band slumping" is primarily dominated by the viscoplastic behavior of the rock and the shear displacements between the lamellae. Thus *UDEC* offers the best way of modeling kink band slumping type failures of rock slopes.

1 PROBLEM STATEMENT

The term "kink band slumping" has been introduced by Kieffer (1989) describing a rock slope failure mechanism leading to normal faulting in the upper part and an S-shaped deformation of rock lamellae dipping steeper than the slope surface in the lower part of the slope (Fig. 1). Zischinsky (1966) and Nemčok, Pašek & Rybář (1972) described similar slope deformations calling them "deep-seated creep" and "Sackung" (Figs. 2-4).

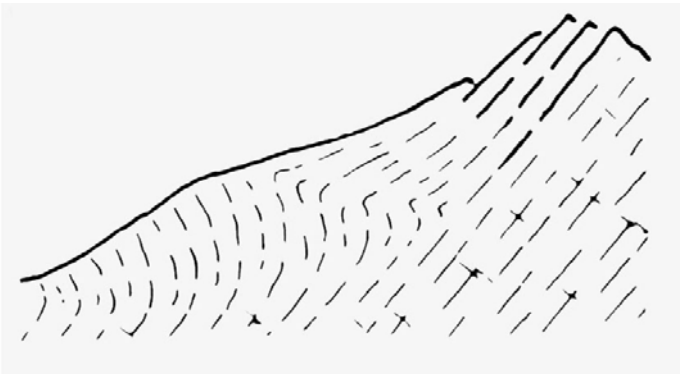

Figure 2. Deep-seated creep grading into sliding in the upper part of the slope described by Nemčok et al. (1972).

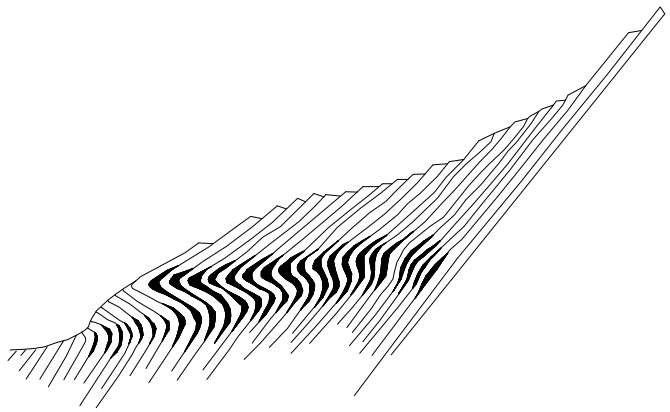

Figure 1. Conceptual model for kink band slumping (Kieffer 1989).

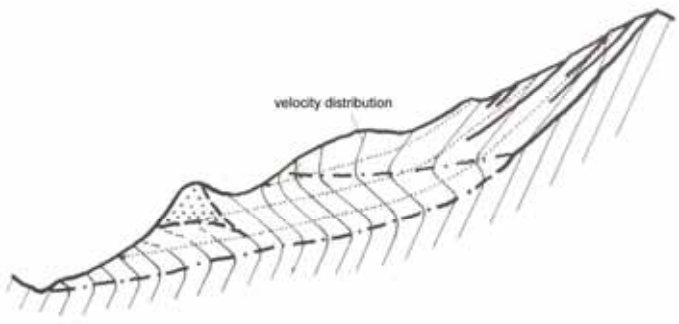

Figure 3. Typical profile of a "Sackung" (Bunzkögele near Matrei, Austria; from: Zischinsky 1966).

Figure 4. Bunzkögele (normal faulting in the upper part of the slope).

Three basic mechanisms have been regarded as the cause of kink band slumping:

1 toppling in the lower part and rock slumping in the upper part of the slope (Kieffer 1989)
2 Bingham creep of the rock due to yielding leading to a type of slope creep (Poisel & Preh 2004)
3 serial buckling of the rock lamellae.

UDEC models built up by columns consisting of discrete blocks and forced to buckling by a hydrostatic head did not show the deformation pattern studied (Fig. 5). Thus buckling could not be considered as the basic mechanism and a *UDEC* model simulating large deformations of the rock due to viscoplastic behavior as well as large shear displacements between the lamellae was set up. The model geometry for the *UDEC* analyses is represented in Figure 6.

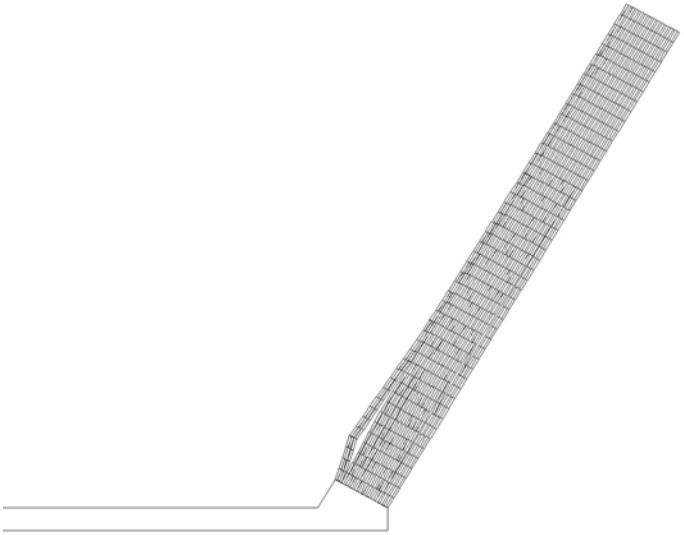

Figure 5. Forced buckling by a hydrostatic head (*UDEC* model).

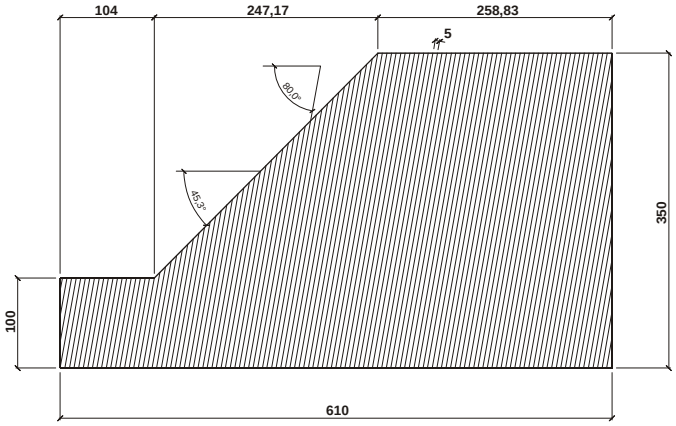

Figure 6. Model geometry.

2 *UDEC* ANALYSES

2.1 *Modeling procedure*

The behavior of the rock was simulated by a Mohr-Coulomb material model with the parameters listed in Table 1. The joints were simulated by the joint constitutive model "joint area contact – Coulomb slip".

The in situ stresses (Fig. 7) were calculated based on pure elastic material behavior. Plastic deformations were prevented by high strength of the rock and the joints. After calculating the in situ stresses, the failure was triggered by reduction of the strength parameters according to the values given in Tables 1 and 2.

Table 1. Material properties – Rock.

ρ [kg/m³]	E [GPa]	ν	c [kPa]	φ [°]	σ_z [kPa]
2.700	6.25	0.25	170	33	30

Table 2. Material properties – Joints.

c [kPa]	φ [°]	σ_z [kPa]
0	10	0

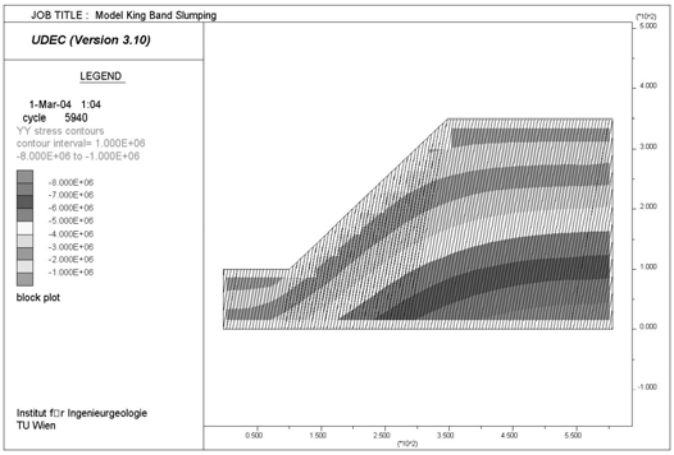

Figure 7. In situ stresses.

2.2 *Boundary conditions*

The boundary conditions have been established by limitation of the degrees of freedom for the grid-points at the model boundaries. Velocities in x-direction have been fixed at the collateral boundaries of the model; velocities in x- and y-direction have been fixed at the base. These boundary conditions have proven as highly useful, when analyzing rock slopes and valley flanks.

2.3 *Calculation of the joint stiffnesses*

UDEC uses a "soft contact" (penetration of blocks possible) in order to model movements normal to a contact plane. If the joint stiffnesses are too high, the solution time of the model increases significantly. On the other hand, problems with the size of the overlap can arise, if the normal stiffness is too low.

Therefore, for mechanical-only calculations joint normal and shear stiffnesses should be kept equal or smaller than ten times the equivalent stiffness of the stiffest neighboring zone in block adjoining the joint:

$$k_n = k_s \le 10 \cdot \left[\max \left[\frac{K + \frac{4}{3} \cdot G}{\Delta z_{min}} \right] \right] \quad (1)$$

where K and G are bulk and shear moduli, respectively, of the block material, and Δz_{min} is the smallest width of the zone adjoining the joint in normal direction.

2.4 *Discretization of the blocks*

In order to simulate the behavior of the block material, the blocks have to be discretized into deformable triangular finite-difference zones. This is generally done by *UDEC* automatically and generates an irregular grid even by axisymmetric blocks. This irregular finite difference grid produces wrong results, when plastic deformations are large. Thus a regular finite-difference grid (diagonally opposed triangular zones, Fig. 8) was used for the analysis of kink band slumping to improve the plastic flow calculation.

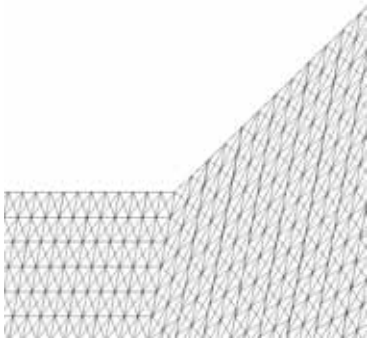

Figure 8. Zoning within the discrete blocks (diagonally opposed triangular zones).

3 RESULTS AND DISCUSSION

Figure 9 shows the failure sequence in the *UDEC* model. At the toe of the slope flexural toppling of the rock lamellae, at the basis of the moving mass S-shaped deformed rock lamellae (Fig. 10) and at the upper slope surface normal faulting along the joints can be observed. Thus the failure zone (transition zone between moving rock mass and rock remaining in place) is determined by yielding rock in the lower part (at yield surface) and by shear displacements on joints in the upper part (Fig. 11).

The analysis did not reveal significant backward rotations of the rock lamellae in the upper part of the slope (Fig. 11). Thus kink band slumping is not a combination of toppling and rock slumping.

The direction of displacements vectors in the upper part of the slope is solely parallel to the steep dipping joints (Fig. 12). This means that pure slumping occurs in the upper part of the slope. No extension and thus no tension cracks, which are typical features of creeping slopes, can be observed in this region. Thus kink band slumping is not a special form of slope creep, but it is an independent mechanism based on the yielding of rock and slipping of joints.

Mechanical models of kink band slumping have to imply both the yielding of the rock material as well as large shear displacements along joints. Therefore kink band slumping can be modeled successfully by *UDEC* and *3DEC*.

REFERENCES

Kieffer, D. S. 1998. Rock Slumping: A Compound Failure Mode of Jointed Hard Rock Slopes. *PhD, University of Berkeley, California*.

Nemčok, A., Pašek, J. & Rybář, J. 1972. Classification of Landslides and Other Mass Movements. *Rock Mechanics.* 4: 71-78.

Poisel, R. & Preh, A. 2004. Rock slope initial failure mechanisms and their mechanical models. *Felsbau* 2 (2004).

Zischinsky, U. 1966. On the deformation of high slopes. In: *Proceedings of the First Congress of the International Society of Rock Mechanics, Lisbon, Portugal,* Volume II: 179-185.

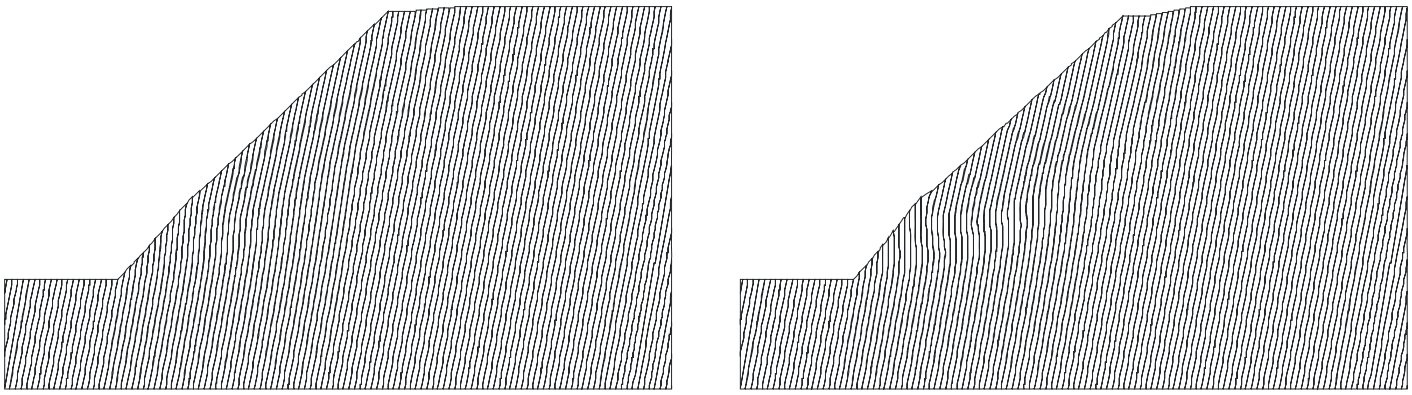

a) b)

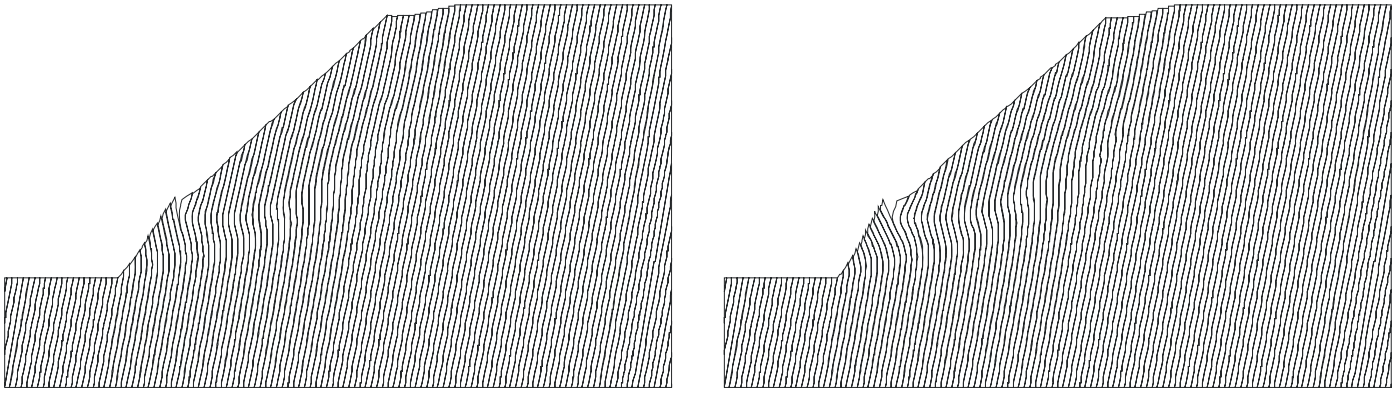

c) d)

Figure 9. Failure of the *UDEC* slope (a–d).

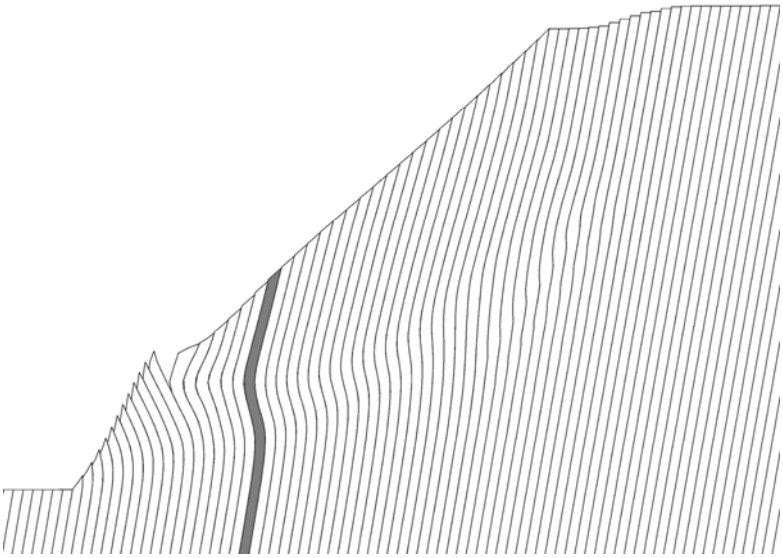

Figure 10. S-shaped deformation of rock lamellae.

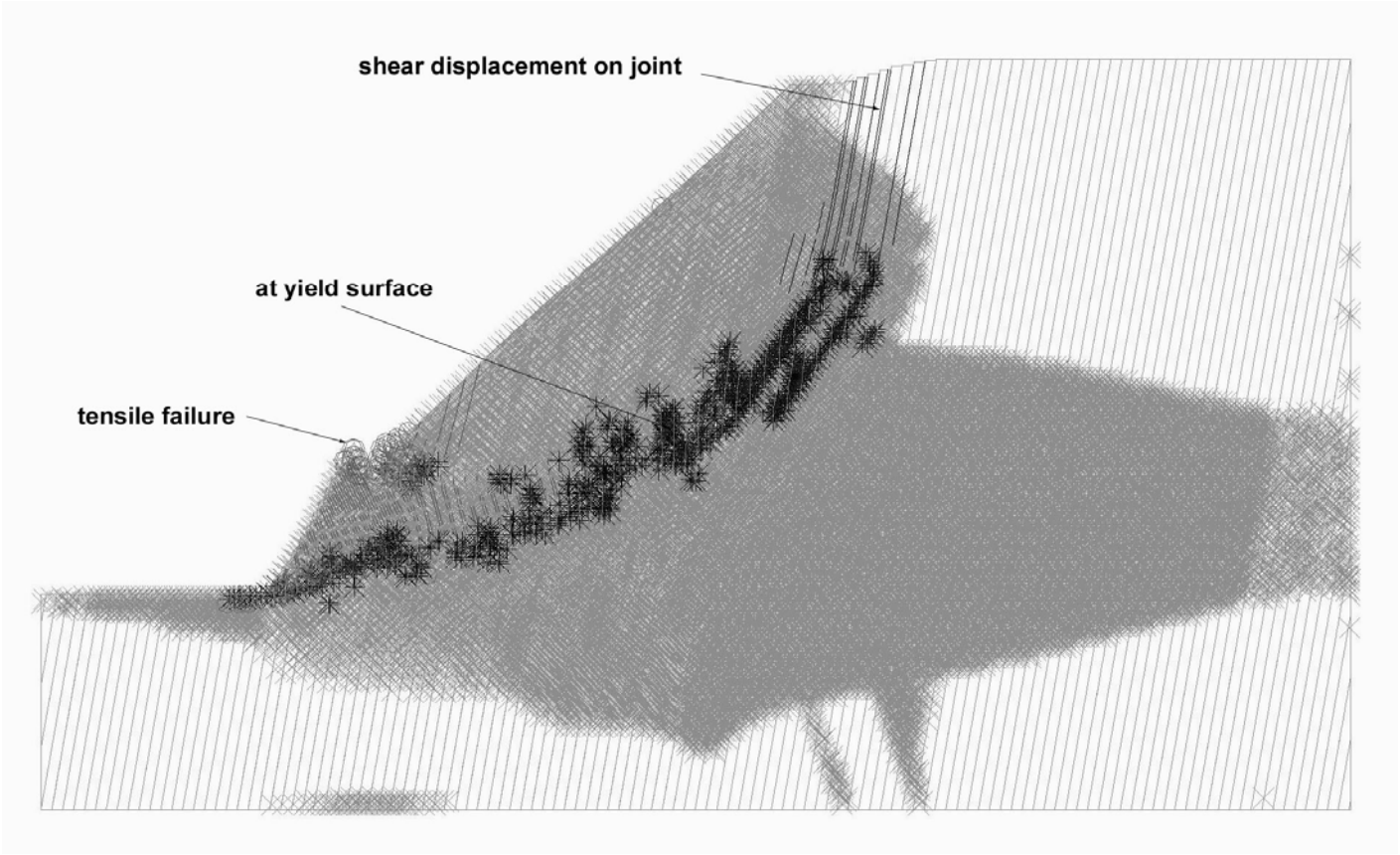

Figure 11. Development of a circular failure surface.

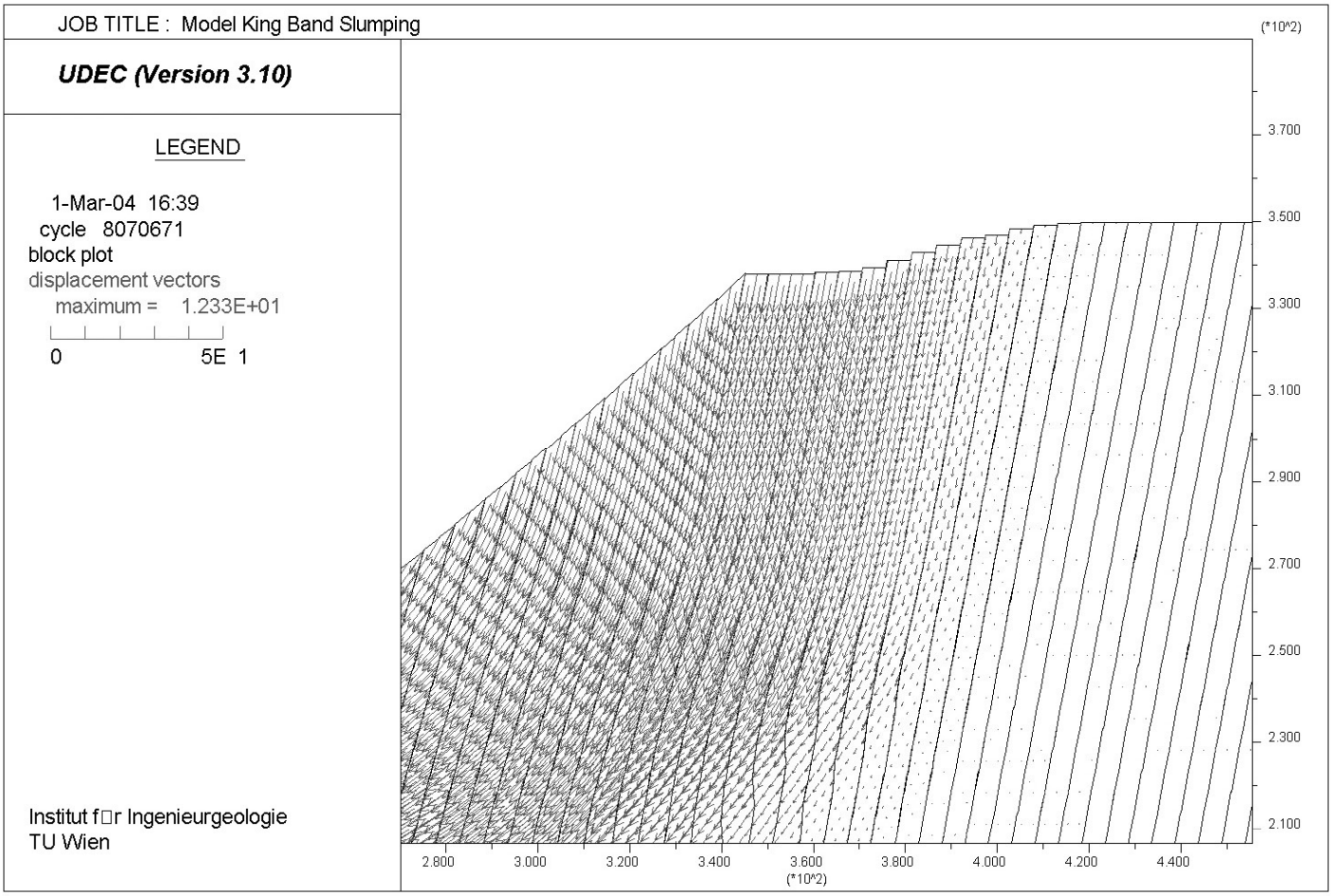

Figure 12. Displacement vectors on the upper part of the slope.